Electronic Supplementary Material (ESI) for Reaction Chemistry & Engineering.

Supporting Information

Highly reproducible, high-yield flow synthesis of gold nanoparticles based on a rational reactor design exploiting the reduction of passivated Au(III)

Luca Panariello[a], Spyridon Damilos[a], Hendrik du Toit[a], Gaowei Wu[a], Anand N.P. Radhakrishnan[a],
Ivan P. Parkin[b], Asterios Gavriilidis[a]

a: Department of Chemical Engineering, University College London, Torrington Place,
London WC1E 7JE, United Kingdom
b: Department of Chemistry, University College London, 20 Gordon Street,
London WC1H 0AJ, United Kingdom

Contents

S1. Calibration of $\mathrm{HAuCl_4}$ concentration against UV-Vis absorbance at $313\ \mathrm{nm}$ 2

S2. TEM micrographs and particle size distributions for particles synthesized via the batch *direct passivated* Turkevich synthesis 3

S3. SPR absorbance and peak wavelength as a function of time in the batch *direct passivated* Turkevich synthesis 5

S4. UV-Vis spectra of $\mathrm{p\_Au(III)}$ at different temperatures 6

S5. TEM micrographs and particle size distributions for particles synthesized via the batch *passivated* Turkevich synthesis with *direct* and *inverse* reactant addition 7

S6. Stability of Au nanoparticles after collection 9

S7. Effect of residence time on characteristics of flow-synthesized Au nanoparticles via the *passivated* Turkevich synthesis 10

S8. Reproducibility of product from batch and flow reactors 11

References 12

S1. Calibration of $HAuCl_4$ concentration against UV-Vis absorbance at 313 nm

The concentration of $AuCl_4^-$ can be related to the absorbance at $313\ nm$.[1,2] At low pH (*e.g.*, $pH = 1$) all the $Au(III)$ in solution is present as $AuCl_4^-$, hence the absorbance at $313\ nm$ can be used to determine the gold precursor conversion.[3] Fig S1 shows the calibration curve used to evaluate the concentration of $Au(III)$ from the absorbance at $313\ nm$, hence the precursor conversion, as explained in detail in the main text. The calibration solutions were prepared by adding the desired volume of $HAuCl_4$ stock ($25\ mM$) to a solution of HCl, with the final pH of ~ 1. Different volumes of stock were used to obtain the UV-Vis spectra of the solutions with different $HAuCl_4$ concentration ranging between $0.125\ mM$ and $0.5\ mM$.

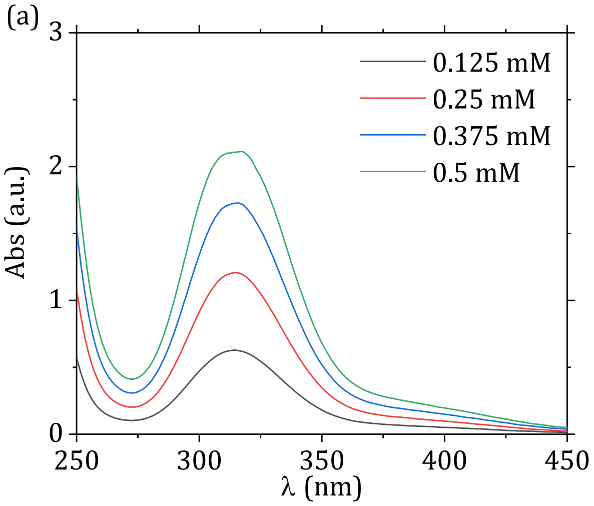

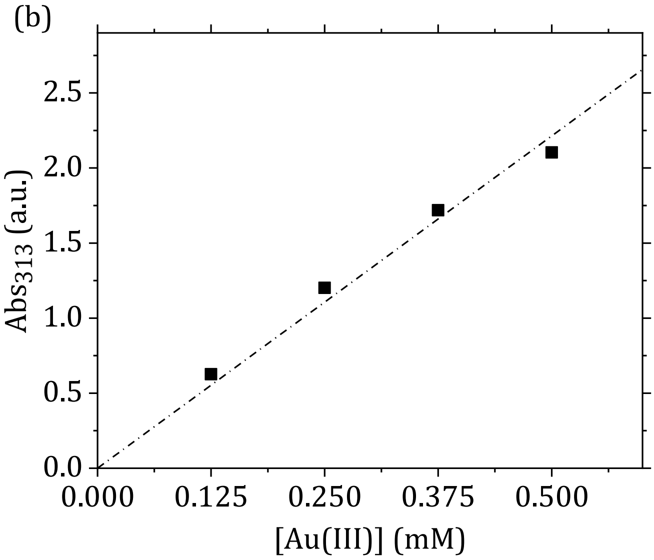

Figure S1. (a) UV-Vis spectra of $Au(III)$ solutions at pH = 1 at various concentrations $HAuCl_4$ and (b) absorbance at 313 nm vs $Au(III)$ concentration. The extinction coefficient determined after calibration is $\varepsilon = 4.43\ L\ mmol^{-1} cm^{-1}$.

S2. TEM micrographs and particle size distributions for particles synthesized via the batch *direct passivated* Turkevich synthesis

This section reports in detail the results (in terms of the particle size distribution) of the *passivated* Turkevich synthesis carried out in batch with *direct* addition of the reactants. The concentration of gold precursor was $[p\_\mathrm{Au(III)}] = 0.2\ \mathrm{mM}$, and the ratios $[\text{citric acid}]/[p\_\mathrm{Au(III)}]$ were in the range 9 - 13.

$[\text{citric acid}]/[p\_\mathrm{Au(III)}] = 9$

$20.3 \pm 2.6\ \mathrm{nm}\ (RSD = 13\%)$

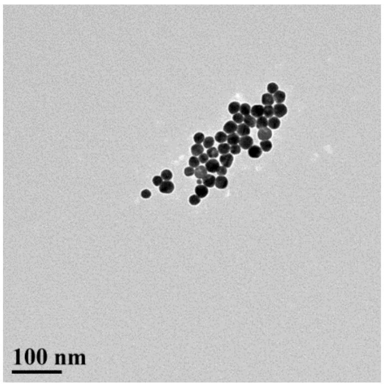

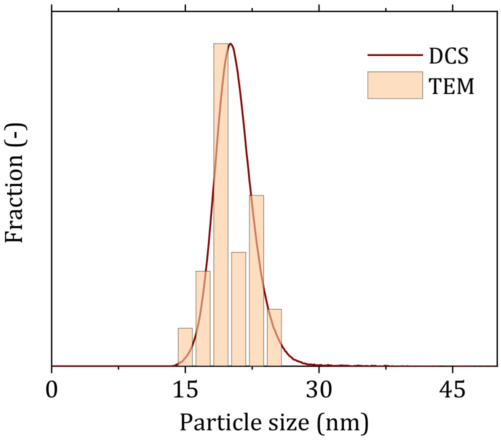

$[\text{citric acid}]/[p\_\mathrm{Au(III)}] = 10$

$15.9 \pm 1.74\ \mathrm{nm}\ (RSD = 11\%)$

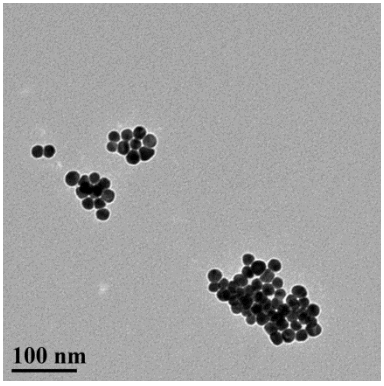

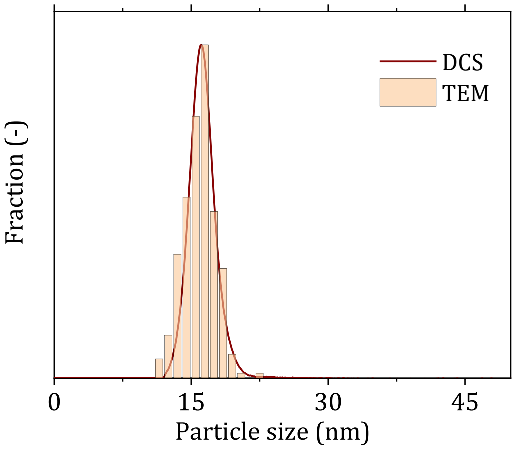

[citric acid]/[p_Au(III)] $= 11$
14 ± 2 nm ($RSD = 13\%$)

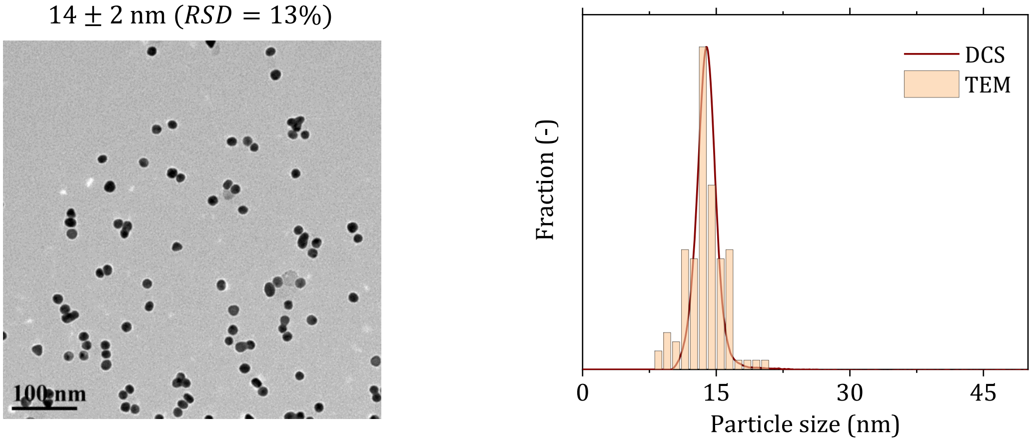

[citric acid]/[p_Au(III)] $= 12$
12.6 ± 1.3 nm ($RSD = 10\%$)

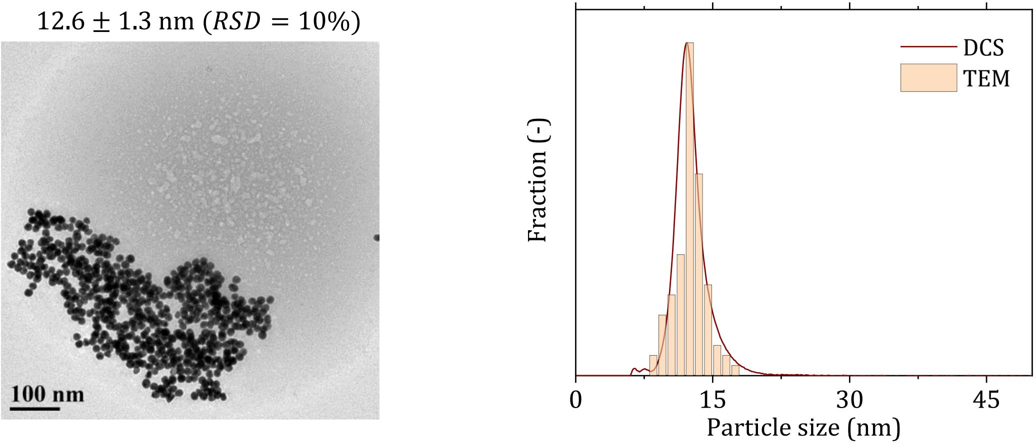

[citric acid]/[p_Au(III)] $= 13$
12.7 ± 1.4 nm ($RSD = 11\%$)

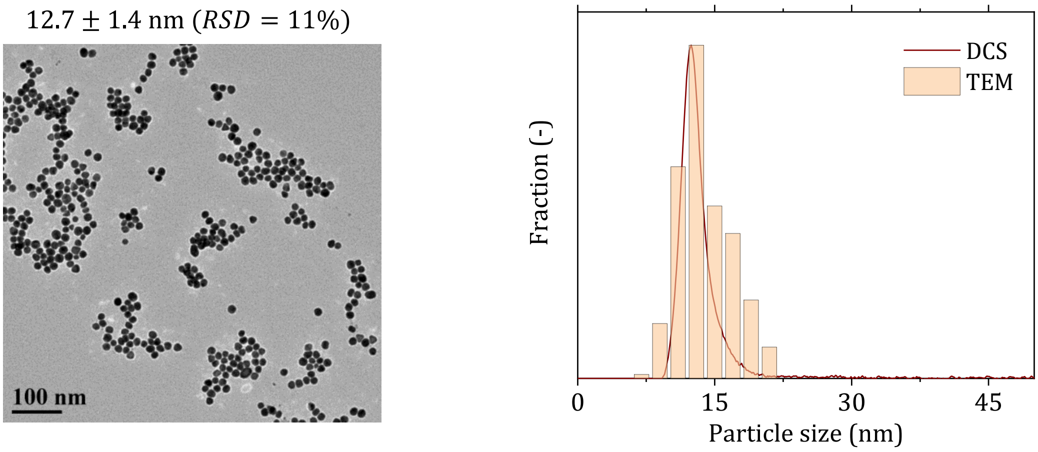

Figure S2. TEM micrographs and corresponding particle size distributions from TEM (bar charts) and DCS (line graphs) of the nanoparticles obtained in batch via the *direct passivated* Turkevich synthesis at different [citric acid]/[p_Au(III)] ratios. In all cases, [p_Au(III)] $= 0.2$ mM and temperature = 90°C. From top to bottom: [citric acid]/[p_Au(III)] = 9, 10, 11, 12 and 13.

S3. SPR absorbance and peak wavelength as a function of time in the batch *direct passivated* Turkevich synthesis

Fig. S3 shows the evolution of the SPR absorbance and peak wavelength during the *passivated Turkevich* method at two different conditions, that is, for [citric acid]/$[p\_\mathrm{Au(III)}]$ equal to 9 and 13, while the other conditions were kept constant ($[p\_\mathrm{Au(III)}] = 0.2\ \mathrm{mM}$ and temperature $= 90°\mathrm{C}$). Increase in the reducing agent concentration led to a decrease in the synthesis pH, as explained in the main text. The curves show the different time scales for the two experiments, with the synthesis carried out at higher reducing agent concentration being faster. In this case, the kinetics of the synthesis become faster by the combined increase in the reducing agent concentration and decrease in pH. Nonetheless, both conditions are qualitatively similar, with a sigmoidal increase in the SPR absorbance (Fig. S3(a)) and a progressive decrease in the SPR peak wavelength from $\sim 550\ \mathrm{nm}$ to $\sim 520\ \mathrm{nm}$ (Fig. S3(b)).

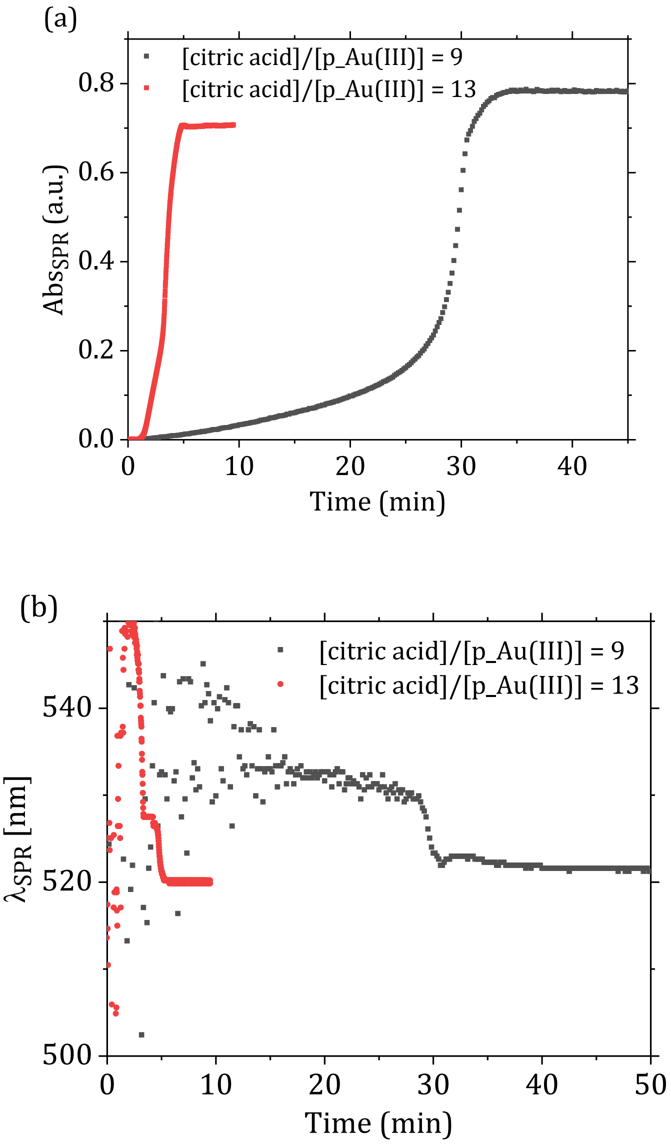

Figure S3. Time-resolved (a) SPR absorbance and (b) SPR peak wavelength for the *direct passivated* Turkevich synthesis, $[p\_\mathrm{Au(III)}] = 0.2\ \mathrm{mM}$, temperature $= 90\ °\mathrm{C}$, [citric acid]/$[p\_\mathrm{Au(III)}]$ ratios of 9 and 13.

S4. UV-Vis spectra of p_Au(III) at different temperatures

Fig. S4 shows that the UV-Vis spectra of p_Au(III) solutions are independent of the temperature in the range 25 - 90°C. This is due to the preparation of the precursor the day before its use with the addition of NaOH, which allowed for the complete conversion of $\mathrm{AuCl_4^-}$ to its more hydroxylated forms $\mathrm{AuCl_{4-x}(OH)_x^-}$. If this was not the case, the increase in temperature should lead to a change in the spectra due to the further conversion $\mathrm{AuCl_4^-}$ into $\mathrm{AuCl_{4-x}(OH)_x^-}$, as the hydroxylated precursor is thermodynamically favoured as the temperature increases.[1]

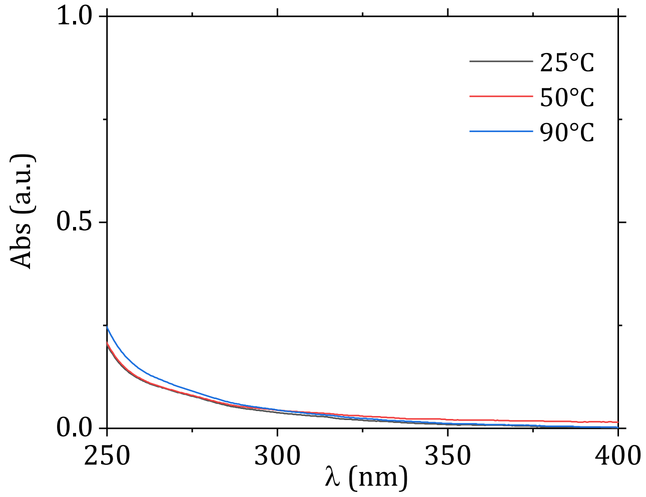

Figure S4. UV-Vis spectra of the p_Au(III) solutions at different temperatures between 25 and 90 °C.

S5. TEM micrographs and particle size distributions for particles synthesized via the batch *passivated* Turkevich synthesis with *direct* and *inverse* reactant addition

This section reports the results obtained when comparing the *passivated* Turkevich synthesis carried out in batch with *direct* and *inverse* reactant addition. Since the synthesis started from a hydroxylated precursor, no change was observed between *direct* and *inverse* synthesis.

Direct reactant addition	*Inverse reactant addition*	*Particle size distribution*
[citric acid]/[$p\_\mathrm{Au(III)}$] $= 9$ 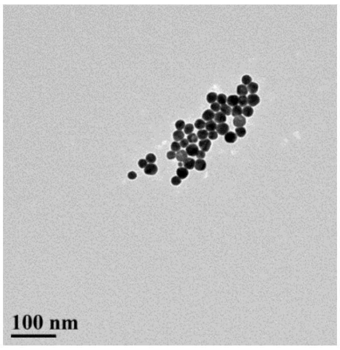 	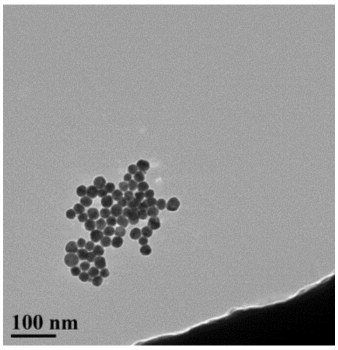 	*direct:* 20.3 ± 2.6 nm ($RSD = 13\%$) *inverse:* 19.6 ± 2.7 nm ($RSD = 14\%$) 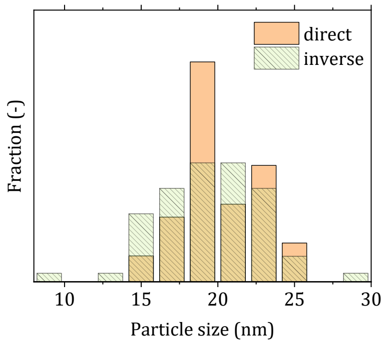
[citric acid]/[$p\_\mathrm{Au(III)}$] $= 10$ 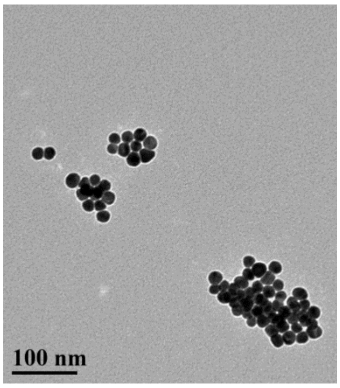 	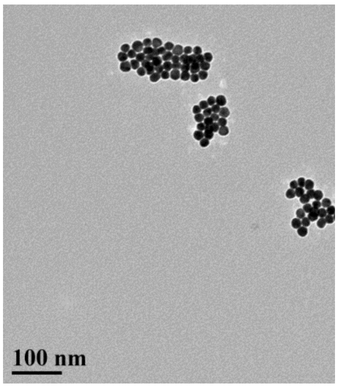 	*direct:* 15.9 ± 1.74 nm ($RSD = 11\%$) *inverse:* 15.9 ± 2.2 nm ($RSD = 14\%$) 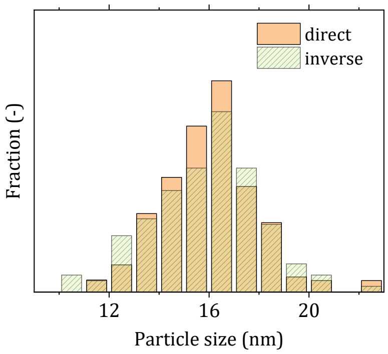

direct: 14 ± 2 nm ($RSD = 13\%$)

inverse: 13.6 ± 1.3 nm ($RSD = 10\%$)

[citric acid]/$[p\_\mathrm{Au(III)}] = 11$

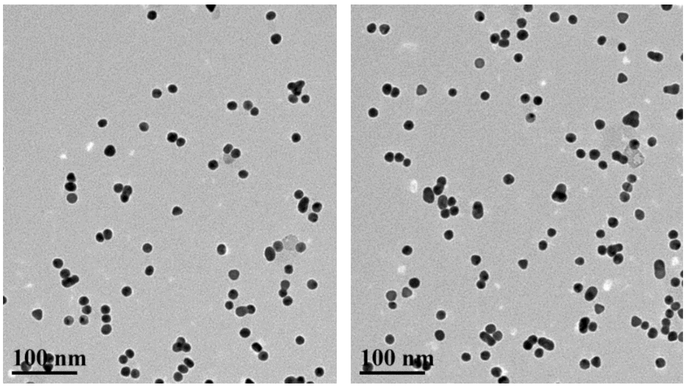

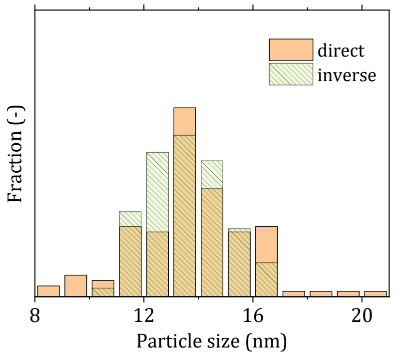

direct: 12.6 ± 1.3 nm ($RSD = 10\%$)

inverse: 12.6 ± 1.5 nm ($RSD = 12\%$)

[citric acid]/$[p\_\mathrm{Au(III)}] = 12$

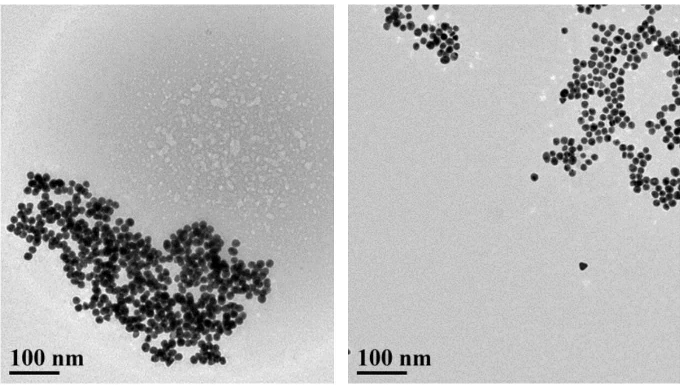

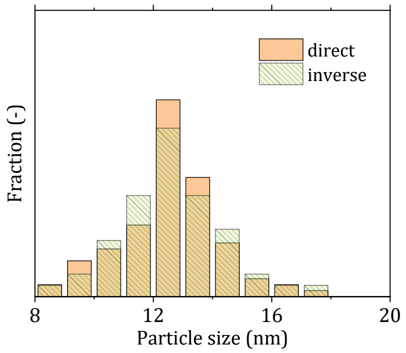

direct: 12.7 ± 1.4 nm ($RSD = 11\%$)

inverse: 12.6 ± 1.3 nm ($RSD = 10\%$)

[citric acid]/$[p\_\mathrm{Au(III)}] = 13$

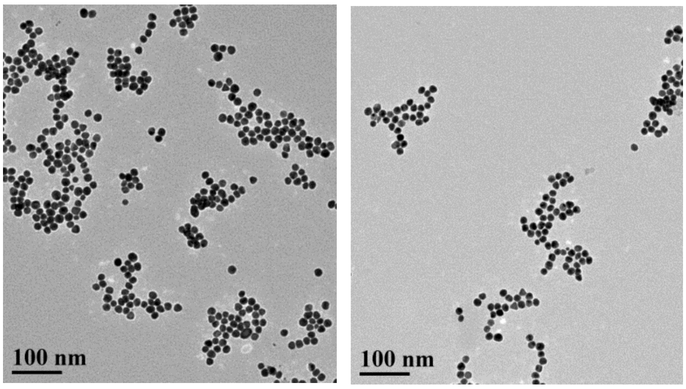

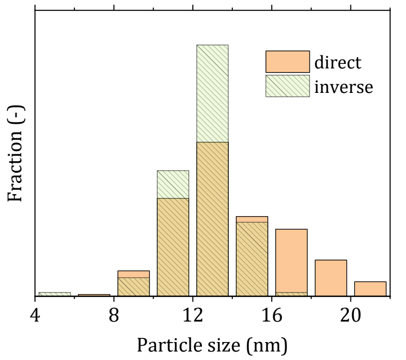

Figure S5. TEM micrographs and corresponding particle size distributions of the nanoparticles obtained in batch via the *direct* and *inverse passivated* Turkevich synthesis at different [citric acid]/$[p\_\mathrm{Au(III)}]$ ratios. In all cases $[p\_\mathrm{Au(III)}] = 0.2$ mM and temperature = 90°C. From top to bottom: [citric acid]/$[p\_\mathrm{Au(III)}]$ = 9, 10, 11, 12 and 13.

S6. Stability of Au nanoparticles after collection

The stability of the flow-synthesized particles ($\tau = 7\ \mathrm{min}$) was tested by checking the change in the UV-Vis spectra of nanoparticle solutions 4 days after the synthesis. The solutions were stored at room temperature in the dark. The spectra did not exhibit any change, suggesting that the reaction was over upon collection.[1]

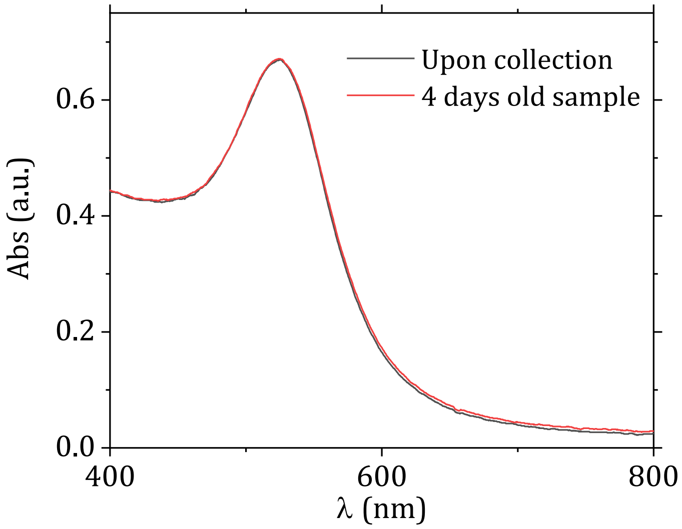

Figure S6. UV-Vis spectra of the flow-synthesized Au nanoparticle solution ($\tau = 7\ \mathrm{min}$) upon collection and after 4 days.

S7. Effect of residence time on characteristics of flow-synthesized Au nanoparticles via the *passivated* Turkevich synthesis

In order to demonstrate that the flow synthesis performed ($[p\_\mathrm{Au(III)}] = 0.2\ \mathrm{mM}$, $[\text{citric acid}]/[p\_\mathrm{Au(III)}] = 12$, temperature $= 90$℃) terminated after $7\ \mathrm{min}$ (as suggested by the UV-Vis data acquired in batch), the synthesis was carried out in the flow reactor at different residence times (4, 7 and $10\ \mathrm{min}$). While the nanoparticles produced at 7 and $10\ \mathrm{min}$ showed no difference, the nanoparticles produced at a residence time of $4\ \mathrm{min}$ showed irregular shape.

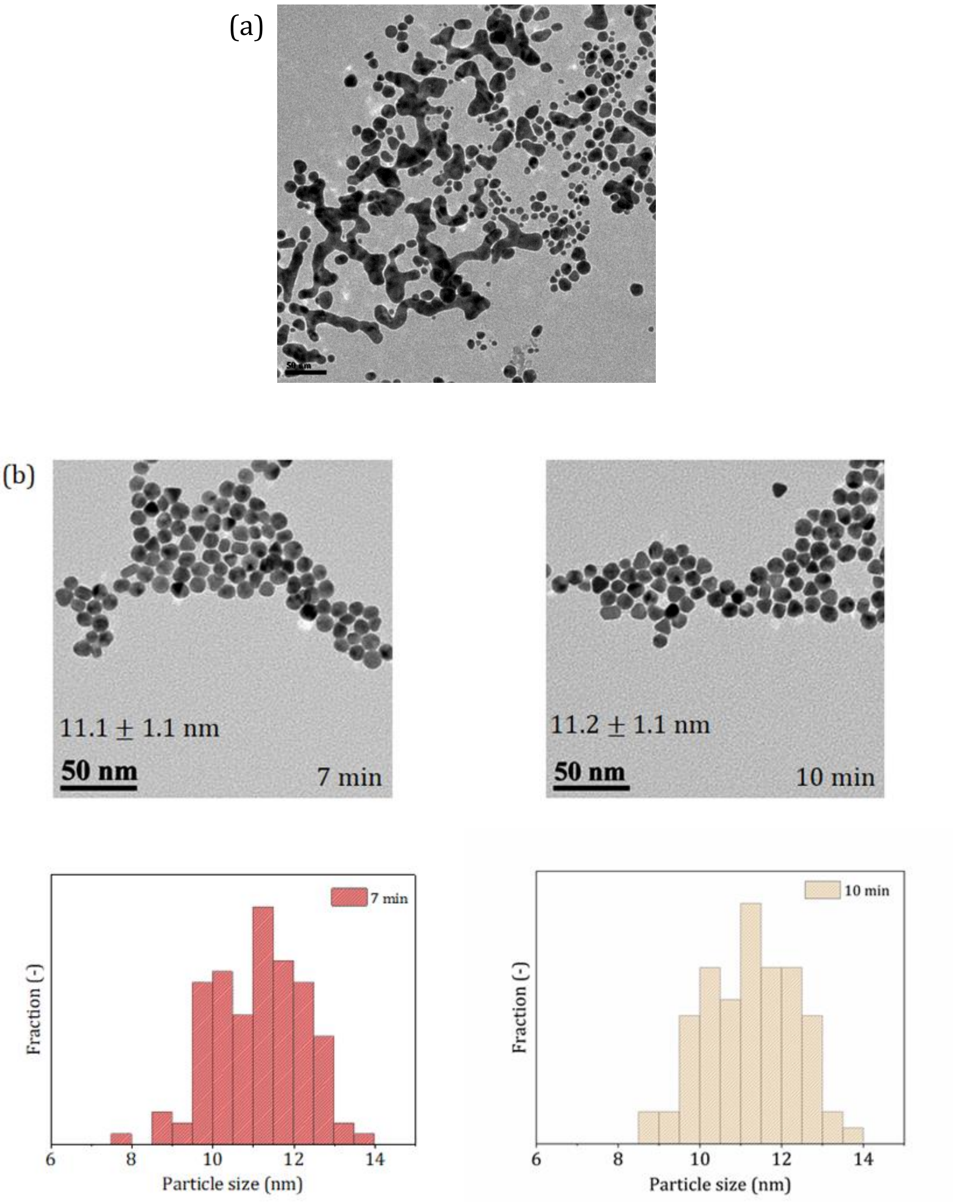

Figure S7. (a) TEM micrograph of the irregular structures formed after the $4\ \mathrm{min}$ residence time synthesis. (b) TEM micrographs and corresponding particle size distributions for the $7\ \mathrm{min}$ and $10\ \mathrm{min}$ residence time syntheses.

S8. Reproducibility of product from batch and flow reactors

Fig. S8 shows the increase in reproducibility of the synthesis carried out in flow compared to that performed in batch. Even though the batch synthesis is highly reproducible (relative standard deviation of the three batch replicates equal to 5%) due to the optimal pH used during the synthesis[4], the reproducibility is further enhanced in flow, with the relative standard deviation of the three replicates performed equal to 2%.

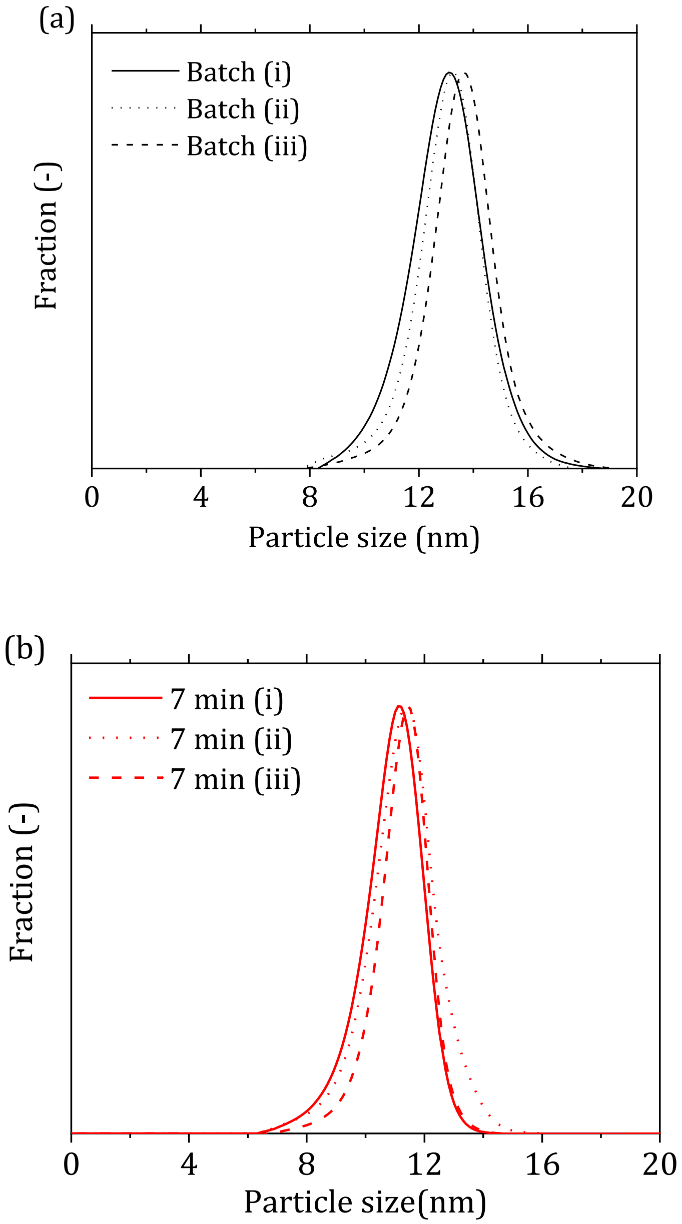

Figure S8. Particle size distributions of the batch- (a) and flow- (b) synthesized Au nanoparticles after different synthesis repeats ($[p\_\mathrm{Au(III)}] = 0.2\ \mathrm{mM}$, [citric acid]/ $[p\_\mathrm{Au(III)}] = 12$, temperature $= 90\ ^\circ\mathrm{C}$, *direct* reactant addition in batch, $\tau = 7\ \mathrm{min}$ in flow). Particle size distributions were determined via DCS.

References

1 M. Wuithschick, A. Birnbaum, S. Witte, M. Sztucki, U. Vainio, N. Pinna, K. Rademann, F. Emmerling, R. Kraehnert and J. Polte, *ACS Nano*, 2015, **9**, 7052–7071.

2 A. Usher, D. C. McPhail and J. Brugger, *Geochim. Cosmochim. Acta*, 2009, **73**, 3359–3380.

3 X. Ji, X. Song, J. Li, Y. Bai, W. Yang and X. Peng, *J. Am. Chem. Soc.*, 2007, **129**, 13939–13948.

4 F. Kettemann, A. Birnbaum, S. Witte, M. Wuithschick, N. Pinna, R. Kraehnert, K. Rademann and J. Polte, *Chem. Mater.*, 2016, **28**, 4072–4081.